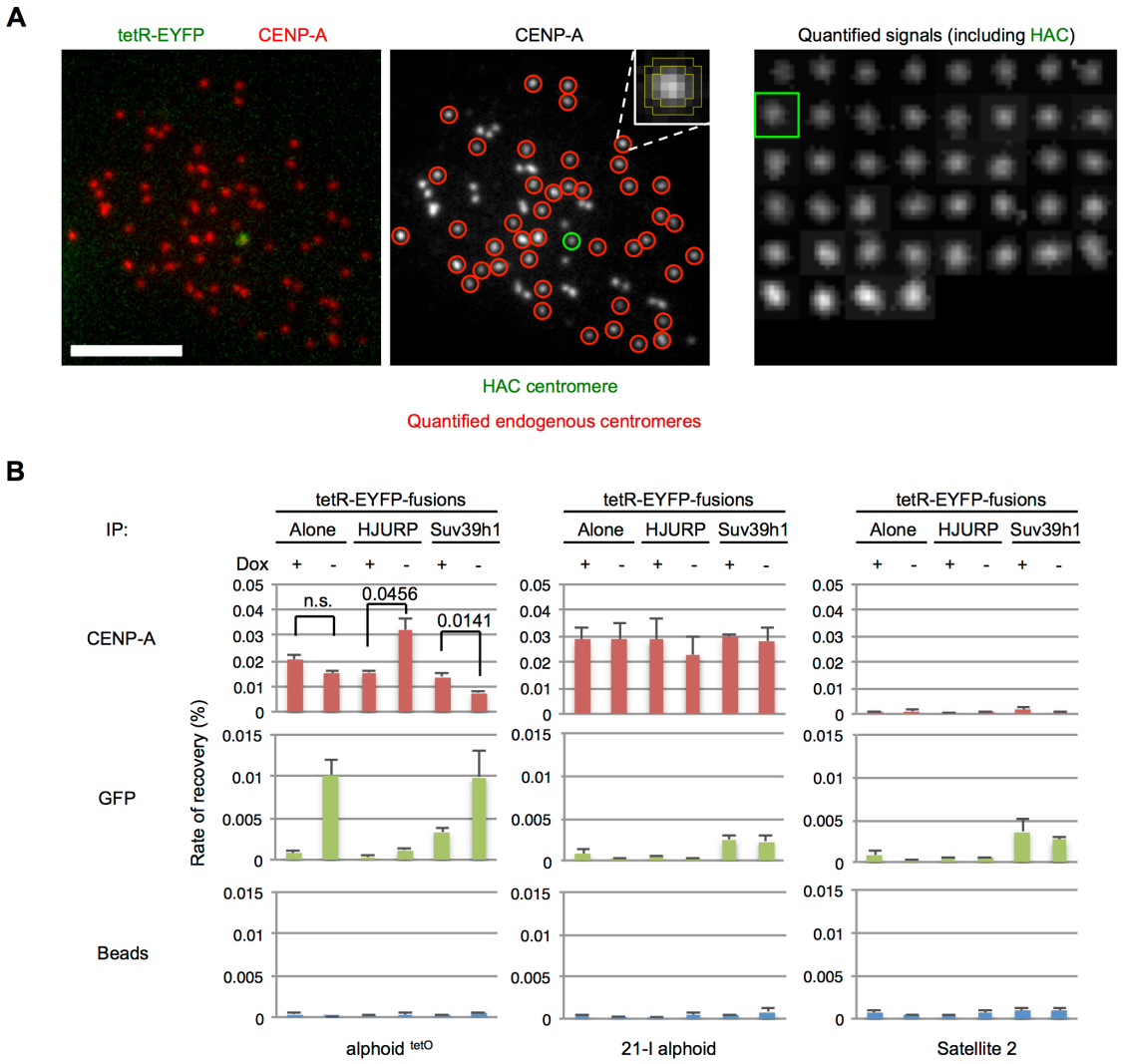

Fig. S1. Quantification and ChIP-qPCR analysis of CENP-A assembly on the HAC

(A) Representative images of HeLa-HAC-2-4 cells transfected with tetR-EYFP-Alone (the same picture as Fig. 1 C). Scale bar, 5 μm. CENP-A signal on the HAC was located by EYFP signal (green circle). Then, endogenous centromeres suitable for quantification (except too close, large or small) were picked up (red circles). Each CENP-A signal was calculated within 5 pixels diameter subtracting background of peripheral pixels (see magnified signal on the middle picture). Then CENP-A signal on the HAC was divided by the average signal of the endogenous centromeres to normalize. Quantified signals including the HAC are displayed in the right panel in order of intensity. The green rectangle indicates the HAC centromere. (B) HeLa-HAC-2-4 cells stably expressing tetR-EYFP-Alone, tetR-EYFP-HJURP or tetR-EYFP-Suv39h1 were cultured with presence or absence of doxycycline (Dox) for four days and harvested

(Dox prevents tetO/tetR binding). The main ChIP procedure was described previously (Ohzeki et al., 2002; 2012), but in this study Dynabeads M-280 Sheep anti-Mouse IgG (Life Technologies) were used instead of Protein G sepharose. Antibodies used in this study are shown in Table S1. The DNA was purified from the immunoprecipitates and quantified by real-time PCR, using the following primer sets: tetOF (5'-CTCTTTTTGTGGAATCTGCAAGTG) and tetOR (5'-TCTATCACTGATAGGGAGAGCTCT) for alphoidtetO, 21alpF (5'-CTAGACAGAAGCCCTCTCAG) and 21alpR (5'-GGGAAGACATTCCCTTTTTCACC) for the 11-mer of chromosome 21 alphoid DNA (21-I alphoid) and Sat2F (5'- GGAATCATCGCATAGAATCGAATGG) and Sat2R (5'- CATTCGAGTCCGTGGATTATTCC) for Satellite 2. Error bars, SEM (standard error of the mean) (n=3). P-values obtained with t-test are indicated (n.s.: not significant).

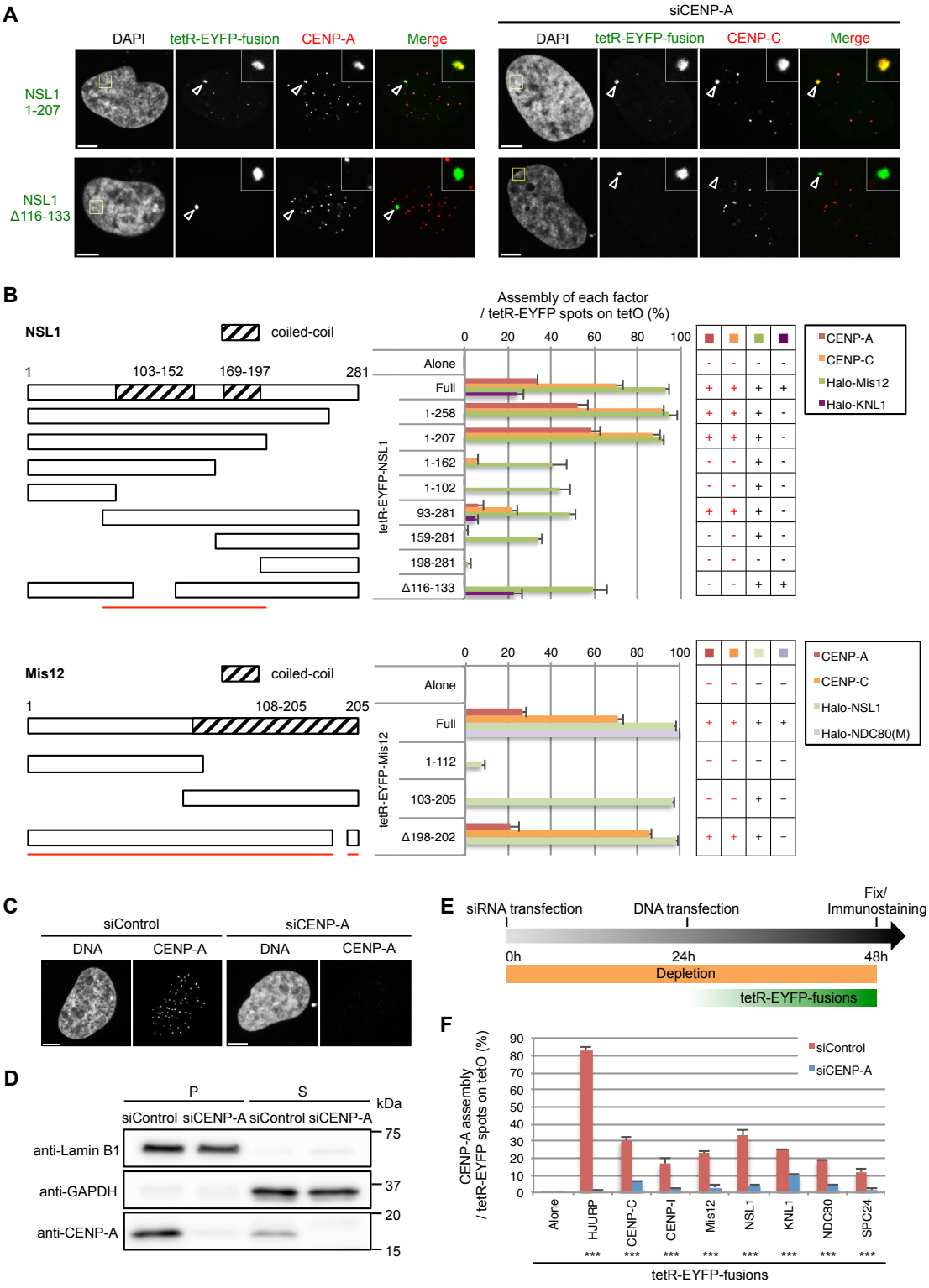

Fig. S2. De novo CENP-A assembly correlates with CENP-C recruitment

All Class I factors are the components of the CCAN or KMN network and interact with one another (Screpanti et al., 2011). We therefore hypothesized that Class I factors

induce de novo CENP-A assembly via recruitment of a few common factors that induce de novo CENP-A assembly. In this case, loss of those common factors would abolish de novo CENP-A assembly activity by Class I factors. (A) Representative images of HeLa-Int-03 cells transfected with indicated tetR-EYFP-NSL1 deletion mutants. Cells were stained with DAPI and anti-CENP-A or CENP-C (red) at 48 or 24 h after transfection, respectively. CENP-C was observed under CENP-A depletion by siRNA transfection followed by plasmid transfection. Arrowheads indicate the ectopic site. Scale bar, 5 μm. (B) Frequency of de novo CENP-A, CENP-C and each Halo-fusion assembly on the ectopic site. Deletion mutants are shown left side. Domains that show relatively high coiled-coil score (calculated with COILS software: http://www.ch.embnet.org/software/COILS_form.html) are indicated by stripes. Red lines show the regions required for de novo CENP-A assembly. siCENP-A was transfected before plasmid transfection except the assay for CENP-A observation. CENP-A, CENP-C or each Halo-fusion signals on tetR-EYFP spot per total tetR-EYFP spots were counted in each sample (n=100 cells for CENP-A and CENP-C, n=50 cells for each Halo-fusion and n=5 cells for Halo-NDC80 (M) which is counted in metaphase cells as Halo-NDC80 spot was rarely observed in interphase cells) at 48 h (CENP-A) or 24 h (CENP-C and Halo-fusions) after transfection. Previous report using in vitro reconstitution (Petrovic et al., 2010) showed that C terminus of NSL1 interacts with KNL1, on the other hand, the C terminus deletion mutant of NSL1 can reconstitute Mis12 complex with other Mis12 components. Similarly, in our in vivo experiment, C terminus deletion mutants of NSL1 (e.g. 1-207 aa) did not recruit KNL1 but Mis12. Additionally, we also showed that these C terminus deletion mutants containing interaction domain with Mis12 can recruit CENP-C and CENP-A without KNL1. (C) Representative images of HeLa-Int-03 cells transfected with indicated siRNAs. Cells were stained with DAPI and anti-CENP-A (A) at 72 h after transfection. Scale bar, 5 μm. (D) The amount of chromosomal (P) and soluble (S) CENP-A were analyzed by immunoblotting using antibodies against Lamin B1 (loading control for P), GAPDH (loading control for S) and CENP-A. Cells were harvested and fractionated at 72 h after each siRNA transfection. (E) Timetable for the experiment (F). HeLa-Int-03 cells were firstly transfected with siRNA. After 24 h incubation, tetR-EYFP-fusion expression

vectors were transfected. Cells were stained with DAPI and anti-CENP-A. (F) Frequency of de novo CENP-A assembly on the ectopic site under each siRNA transfection. Indicated tetR-EYFP-fusion proteins were transfected after siRNA transfection. CENP-A signals on the tetR-EYFP spot per total tetR-EYFP spots were counted in each sample (n=100 cells) at 48 h after plasmid transfection. Asterisks indicate significant differences between indicated siRNAs. ***: P<0.001 (Fisher's exact test). Error bar, SEM. (N=3)

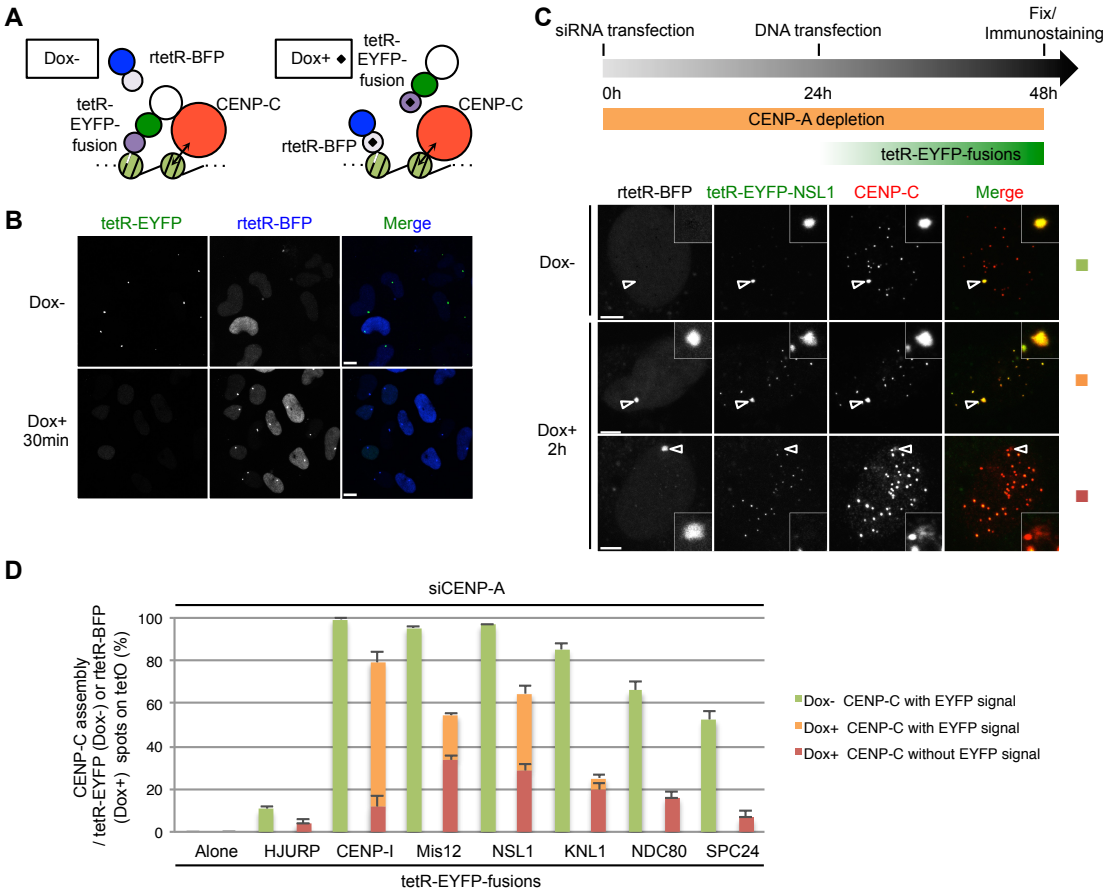

Fig. S3. CENP-C retains binding to chromatin in the absence of CENP-A

(A) A schematic drawing of detection of chromatin bound CENP-C. CENP-C binding to chromatin continues after dissociation of tetR-EYFP-fusion by doxycycline (Dox) treatment. Reverse tetR (rtetR) binds to tetO by Dox treatment, which visualizes ectopic site. (B) Representative images of HeLa-Int-03 cells co-transfected with tetR-EYFP (green) and rtetR-BFP (blue). Cells were treated with or without Dox for 30 min before fixation 48 h after transfection. tetR-EYFP dissociated in 30 min under Dox treatment. Scale bar, 10 µm. (C) Representative images of HeLa-Int-03 cells co-transfected with tetR-EYFP-NSL1 and rtetR-BFP (blue) after siCENP-A transfection. Cells were stained with DAPI and anti-CENP-C (red) at 48 h after plasmid transfection. Cells were treated with or without Dox for 2 h before fixation. Arrowheads indicate the ectopic site. Scale bar, 5 µm. (D) Frequency of CENP-C assembly on the ectopic site. Indicated tetR-EYFP-fusion proteins and rtetR-BFP expressing plasmids were co-transfected after siCENP-A transfection. CENP-C signals on the tetR-EYFP (Dox-) or the rtetR-BFP (Dox+) spot per total spots were counted in each sample (n=50 cells) fixed at 48 h after

plasmid transfection. Under Dox+ condition two types of spots, which show both EYFP and CENP-C signals or only CENP-C signals on the rtetR-BFP spots, were counted. Error bar, SEM. (N=3)

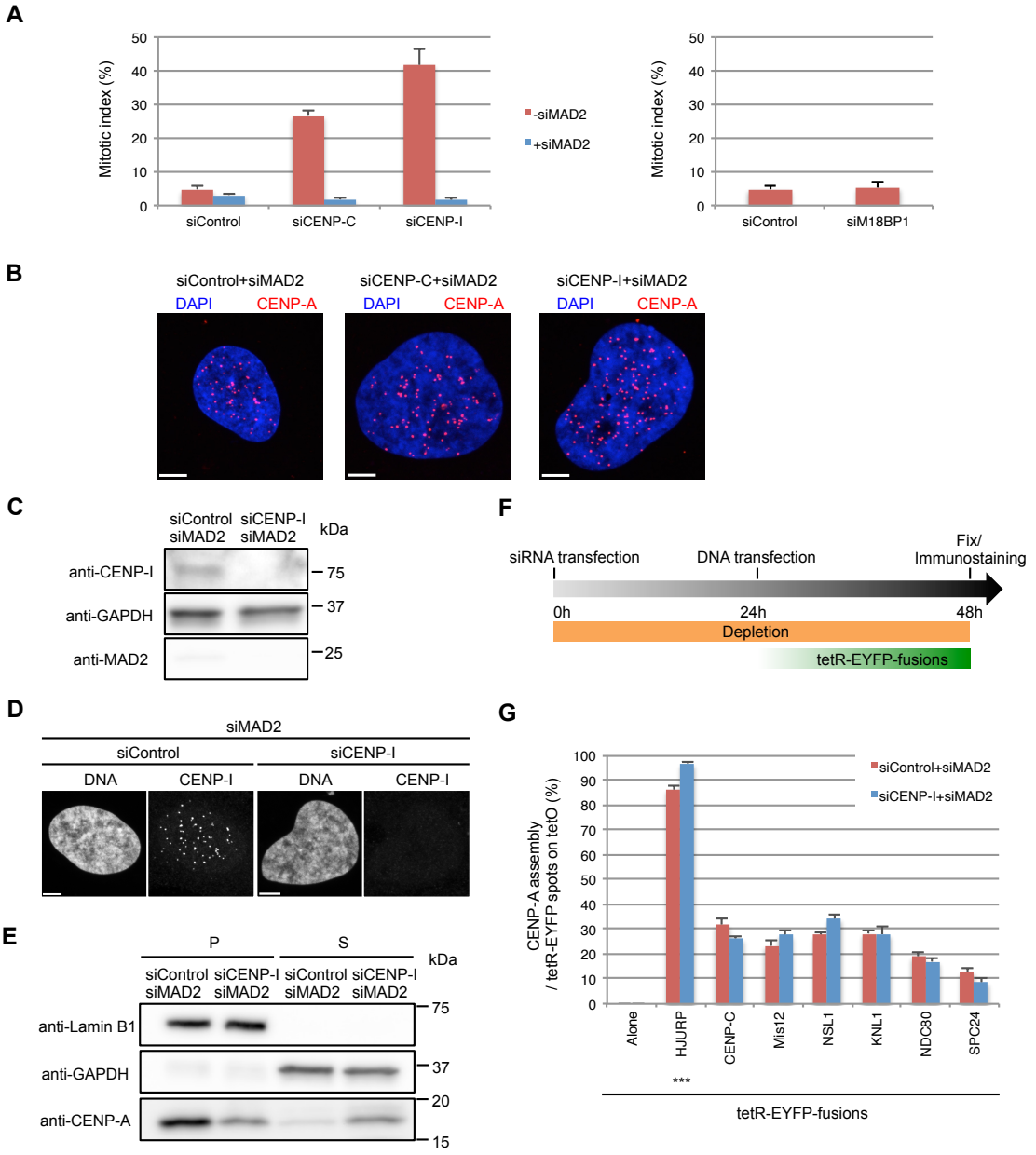

Fig. S4. De novo CENP-A assembly on the ectopic site under CENP-I depletion

(A) MAD2 depletion suppresses mitotic arrest caused by CENP-C or CENP-I depletion**.** HeLa-Int-03 cells were transfected with indicated siRNAs. Cells were fixed at 72 h after transfection. Graph shows mitotic index counted in each sample (n=200 cells). Error bar, SEM. (N=3) Mitotic arrest caused by CENP-C or CENP-I depletion was suppressed by MAD2 depletion. M18BP1 depletion did not cause mitotic arrest. (B) Representative images of HeLa-Int-03 cells co-transfected with siMAD2 and siControl, siCENP-C or siCENP-I. Cells were stained with DAPI and anti-CENP-A (red) at 72 h after transfection. Large nuclei presumably caused by the slippage from the mitotic arrest

were frequently observed in the cells transfected with siMAD2 and siCENP-C or siCENP-I. Scale bar, 5 μm. (C) CENP-I and MAD2 expression were analyzed by immunoblotting using antibodies against CENP-I, GAPDH (loading control) and MAD2. Cells were harvested at 72 h after siRNA transfection. (D) Representative images of HeLa-Int-03 cells transfected with indicated siRNAs. Cells were stained with DAPI and anti-CENP-I at 72 h after transfection. Scale bar, 5 μm. (E) The amount of chromosomal (P) and soluble (S) CENP-A were analyzed by immunoblotting using antibodies against Lamin B1 (loading control for P), GAPDH (loading control for S) and CENP-A. Cells were harvested and fractionated at 72 h after each siRNA transfection. (F) Timetable for the experiment (G). HeLa-Int-03 cells were firstly transfected with siRNA. After 24 h incubation, tetR-EYFP-fusion expression vectors were transfected. Cells were stained with DAPI and anti-CENP-A. (G) Frequency of de novo CENP-A assembly on the ectopic site under each siRNA transfection. Indicated tetR-EYFP-fusion proteins were transfected after siRNA transfection. CENP-A signals on the tetR-EYFP spot per total tetR-EYFP spots were counted in each sample (n=100 cells) at 48 h after plasmid transfection. Asterisks indicate significant differences between indicated siRNAs. The data of siControl+siMAD2 is the same as Fig. 5 J. ***: $P<0.001$ (Fisher's exact test). Error bar, SEM. (N=3)

Table S1. Antibodies used in this study

Antibodies	Catalog number	Antibody produced in	Usage (Dilusion)
anti-CENP-A (A1) (Ohzeki et al., 2002)	None	Mouse	Immuno-staining (1μg/ml), ChIP (5μg/IP)
anti-CENP-A (6F2) (Kind gift of Kinya Yoda)	None	Rat	WB (1/10000)
anti-CENP-C	MBL, PD030	Guinea pig	Immuno-staining (1/2000), WB (1/10000)
anti-CENP-I	MBL, PD032	Rat	Immuno-staining (1/500), WB (1/5000)
anti-M18BP1	Novus Biologicals, NBP1-47290	Rabbit	WB (1/20000)
anti-MAD2	BD Transduction Laboratories, 610679	Mouse	WB (1/10000)
anti-GFP	Roche, 11814460001	Mouse	ChIP (2μg/IP)
anti-□-tubulin	Abcam, ab6160	Rat	Immuno-staining (1/10000)
anti-Lamin B1	MBL, PM064	Rabbit	WB (1/100000)
anti-GAPDH HRP-conjugate	Abcam, ab9484	Goat	WB (1/200000)
anti-mouse IgG HRP-conjugate	Bio-rad, #170-6516	Goat	WB (1/20000)
anti-rabbit IgG HRP-conjugate	Bio-rad, #170-6515	Goat	WB (1/20000)
anti-rat IgG HRP-conjugate	Santa Cruz, sc-2065	Goat	WB (1/20000)
anti-guinea pig IgG HRP-conjugated	Santa Cruz, sc-2438	Goat	WB (1/20000)
anti-mouse IgG Alexa Fluor 594-conjugate	life technologies, A-11032	Goat	Immuno-staining (1/1000)
anti-rat IgG Alexa Fluor 488-conjugate	life technologies, A-11006	Goat	Immuno-staining (1/1000)
anti-rat IgG Alexa Fluor 594-conjugate	life technologies, A-11007	Goat	Immuno-staining (1/1000)
anti-guinea pig IgG DyLight 594-conjugate	Abcam, ab96961	Goat	Immuno-staining (1/500)